ORIGINAL RESEARCH

Retinal Shape-Based Classification of Retinal Detachment and Posterior Vitreous Detachment Eyes

Stewart R. Lake · Murk J. Bottema · Keryn A. Williams ·

Tyra Lange · Karen J. Reynolds

ABSTRACT

Introduction: Retinal detachment is a sight-threatening emergency, with more than half of those affected suffering permanent visual impairment. A diagnostic test to identify eyes at risk before vision is threatened would enable exploration of prophylactic treatment. This report presents the use of irregularities in retinal shape, quantified from optical coherence tomography (OCT) images, as a biomarker for retinal detachment.

Methods: OCT images were taken from posterior and mid-peripheral retina of 264 individuals [97 after a posterior vitreous detachment (PVD), 99 after vitrectomy for retinal detachment and 68 after laser for a retinal tear]. Diagnoses were taken from history, examination and OCT. Retinal irregularity was quantified in the frequency domain, and the distribution of irregularity across the regions of the eye was explored to identify features exhibiting the greatest difference between retinal detachment and PVD eyes. Two of these features plus axial length were used to train a quadratic discriminant analysis classifier. Classifier performance was assessed by its sensitivity and specificity in identifying retinal detachment eyes and visualised with a receiver operating characteristic (ROC) curve.

Results: Validation set specificity was 84% (44/52 PVD eyes correctly labelled) and sensitivity 35% (23/64 retinal detachment eyes identified, $p = 0.02$). Area under the ROC curve was 0.75 (95% confidence intervals 0.58–0.85). Retinal detachment eyes were significantly more irregular than PVD eyes in the superior retina (0.70 mm versus 0.49 mm, $p < 0.05$) and supero-temporal retina (1.12 mm versus 0.80 mm, $p < 0.05$). Lower sensitivity (16/68, 24%) was seen for eyes with a retinal tear without detachment, that were intermediate in size between retinal detachment and PVD eyes. Axial length on its own was a poor classifier. Neither irregularity nor classification were affected by surgery for retinal detachment or the development of PVD.

Conclusions: The classifier identified 1/3 of retinal detachment eyes in this sample. In future work, these features can be evaluated as a test for retinal detachment prior to PVD.

S. R. Lake (✉) · K. A. Williams
Flinders Institute for Health and Medical Research, Flinders University, Adelaide, Australia
e-mail: stewart.lake@flinders.edu.au

S. R. Lake · M. J. Bottema · T. Lange · K. J. Reynolds
Medical Device Research Institute, College of Science and Engineering, Flinders University, Adelaide, Australia

Key Summary Points

Why perform this study?

Retinal detachment is a sight-threatening emergency where more than half of those affected are left with permanently impaired vision

Prophylaxis has been demonstrated to be effective, but for most cases there is no way of identifying who will be affected

This study was looking for a test that could identify which eyes will be affected by retinal detachment

What was learned?

There are differences in peripheral retinal shape measured with optical coherence tomography between post hoc eyes treated by vitrectomy for retinal detachment and those with a posterior vitreous detachment

These differences do not appear to be affected by surgery or posterior vitreous detachment

INTRODUCTION

Rhegmatogenous retinal detachment (hereafter retinal detachment) is a sight-threatening emergency. Most cases develop from a retinal tear formed when posterior vitreous detachment (PVD) occurs, typically after the fourth decade of life. Retinal detachment affects approximately 1% of the population [1–3], with the majority of eyes experiencing an uncomplicated PVD without formation of a retinal tear. Even with successful surgery, more than half of those affected by retinal detachment lose vision [4–7]. In the less than 1% of retinal detachment cases known to be at high risk due to syndromic disease (Type 1 Stickler syndrome) or severe fellow eye disease (giant retinal tears), early prophylactic laser treatment prior to PVD has led to a five to tenfold reduction in vision loss [8–10]. There is at present no method to predict which eyes will develop a retinal tear or detachment prior to posterior hyaloid separation, although risk of retinal detachment is known to rise with increasing myopia [11]. Therefore, there is a need for a clinical test to identify eyes that will develop retinal detachment. Any increase in the number of eyes identified as at risk would create opportunities to further explore prevention.

Retinal irregularity is a biomarker that correlates with axial length, the primary determinant of myopia. Measured with optical coherence tomography (OCT), it is defined as the residual retinal shape after removal of the best fit (second order polynomial) curve from the retinal contour, where the retinal contour is the path of the retinal pigment epithelium across the OCT (see Supplementary information 1). This is often more irregular in the mid-peripheral retina than would be expected from examination of the macula [12]. As both retinal irregularity and risk of retinal detachment increase with increasing myopia, the possibility of the former being a biomarker for the latter motivated the investigation reported herein. The ultimate goal is to develop a test that can predict retinal detachment.

This paper reports the systematic measurement of the retinal irregularity of posterior and mid-peripheral retina in eyes that have experienced either a retinal detachment, PVD or retinal tear without detachment. Retinal irregularity was quantified through fast Fourier transformation, which describes the irregularity by deconstructing it into partitions (bins) in a spectrum of sine waves. The regions of the eye with the greatest differences in irregularity between PVD and retinal detachment were identified. These were combined with axial length to train a machine learning classifier to identify eyes that had a retinal detachment from a mixed group of retinal detachment and PVD eyes. The classifier was tested further with an independent validation set of eyes with a

Table 1 Participant demographics

		Age ± SD (years)	AL ± SD (mm)
PVD	Training set (n = 45)	64.5 ± 6.6	24.08 ± 1.10
	Test set (n = 52)	66.2 ± 5.1	24.36 ± 1.24
	All (n = 97)	65.3* ± 5.9	24.23† ± 1.18
Retinal detachment	Training set (n = 35)	63.1 ± 7.4	25.10 ± 0.98
	Test set (n = 64)	61.4 ± 9.5	25.09 ± 1.33
	All (n = 99)	62.1* ± 8.8	25.09† ± 1.21
Retinal tear	All (n = 68)	64.1‡§ ± 6.2	24.62‖# ± 1.28

Mean age and axial length (AL) for the three groups, subdivided where appropriate into training set and validation set. Age is in years, with axial length in millimeters. Comparison of all retinal detachment eyes to all PVD eyes: *age: $p = 0.0027$, † axial length: $p < 0.005$ (0.00000115). RT eyes to all PVD eyes: ‡age: $p = 0.18$, ‖axial length: $p = 0.04$. RT eyes to all retinal detachment eyes. §Age: $p = 0.09$, #axial length: $p = 0.01$ (two sample t-test). *RT* retinal tear eyes, *PVD* posterior vitreous detachment eyes, *SD* standard deviation

retinal tear. Finally, evidence is presented in the section "The effect of PVD and surgery on retinal shape" that retinal irregularity is not affected by retinal detachment surgery or development of PVD.

METHODS

Study Participants

Individuals were recruited from ophthalmic clinics of a tertiary care hospital (Flinders Medical Centre) and a private ophthalmic practice (Eyemedics), in Adelaide, South Australia, following examination by a retinal specialist. Those with a PVD or retinal tear were imaged within 2 months of presentation. Retinal detachment eyes were imaged within 4 months of diagnosis in the post-operative period after retinal reattachment was confirmed and intraocular gas had dissipated. There were 264 participant eyes from 264 individuals in three groups: those who had undergone vitrectomy without scleral buckling for a PVD-associated retinal detachment (n = 99), those who had presented with an acute symptomatic PVD with complete separation of the posterior hyaloid from the macula and optic disc confirmed by OCT (n = 97) and those with an acute symptomatic PVD-associated retinal tear that was treated by laser (n = 68). There were 134 right eyes and 130 left eyes, with 159 male and 105 female participants. Age ranged from 43 to 83 years, with axial length 21.11–28.09 mm. Of those that had a retinal detachment, 45 were macula on, 43 macula off and 3 macula split at time of surgery, with missing data for 8. Patient demographics are presented in Table 1. The study was approved by the Southern Adelaide
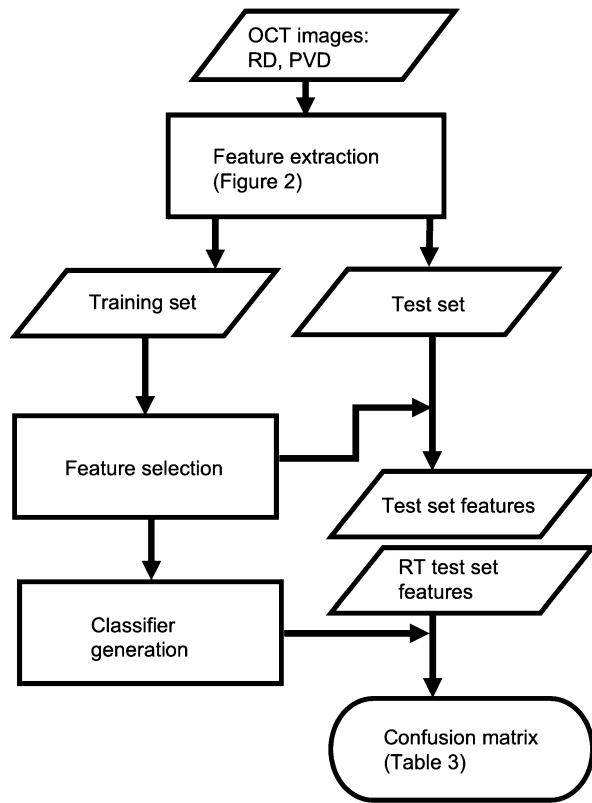
Fig. 1 Flow chart. The data set of retinal detachment (RD) and PVD eyes was split into training and testing sets. Shape features were extracted from the training set images (Fig. 2) and explored to find useful differences between retinal detachment and PVD eyes. These were combined with axial length to train a classifier. The classifier was tested with the validation set of retinal detachment and PVD eyes, and a separate validation set of retinal tear eyes. Results are presented in a confusion matrix in Table 3

Local Health Network Human Research Ethics Committee and was performed in accordance with the tenets of the Declaration of Helsinki. Prior written informed consent was obtained from all participants.

Imaging and Image Processing

Eyes underwent systematic imaging of the posterior pole and mid-periphery of the retina using the Zeiss Cirrus 5000 spectral-domain OCT (Carl Zeiss Meditec AG, Germany). After pupil dilation with one drop each of tropicamide 1% and phenylephrine 2.5% (Bausch &

Fig. 2 Shape analysis and feature extraction. The retinal ▶ shape (taken from the retinal pigment epithelial line) in the B scan (i), is plotted in (ii). The middle figure (iii) shows the residual left after subtraction of the best fit quadratic curve. Figure (iv) is the Fourier transform of (iii) and describes the retinal irregularity in the frequency domain. The 30 lowest frequency bins are magnified in (v). The difference between an individual B scan irregularity [dotted line in (vi)] and the average B scan irregularity [solid line in (vi)] was used for analysis (Supplementary information 1). Each vertical coloured bar represents the contribution of a range of frequencies (a bin) to the irregularity and is used for analysis of shape. Note the B scan image (i) is shown as presented in the clinic, and it is not uncommon for mid-peripheral retina to be as irregular as this. The true aspect ratio is 9 mm (wide) × 2 mm (deep)

Lomb, Chatswood, Australia), OCT cubes of 21 parallel B scans of 9 mm length and spaced by 0.4 mm were captured (HD21 cube protocol). Zeiss OCT machines do not perform pre-processing image flattening, so that retinal irregularity is preserved in the B scan. OCT cubes were grouped into 17 regions: the macula, and two OCT cubes in each direction of gaze (up, down, left, right, up left, up right, down left, down right), one more anterior to the other (labelled post-equatorial and peri-macular, respectively). Axial length was measured via partial coherence interferometry with the Zeiss IOLMaster (Carl Zeiss Meditec AG, Germany).

The retinal irregularity for each scan was quantified in the frequency domain, so that the shape was described by a vector of 30 bin values from the spectrum of sine waves (Fig. 2). Measurement of retinal shape and quantification of irregularity was performed with code written for this study in MATLAB (The MathWorks, Inc., Natick, MA) and is described in Supplementary material 1.

Feature Selection and Development of a Retinal Shape Classifier

Potential variables for classification are here called features. Classification was performed using a standard process of identifying features that appeared best able to separate the two
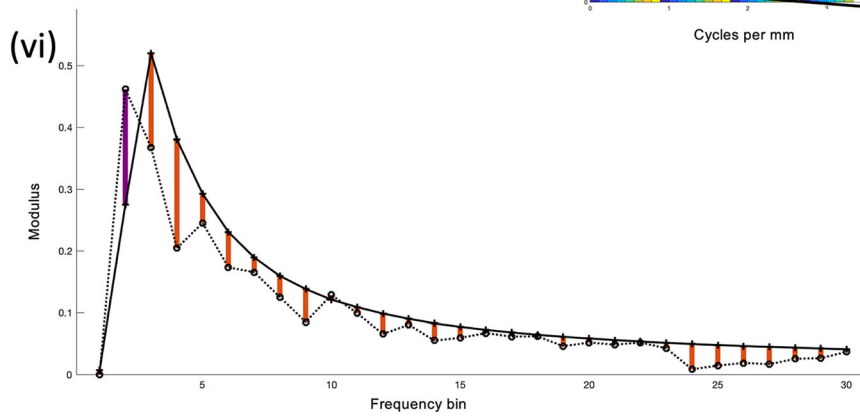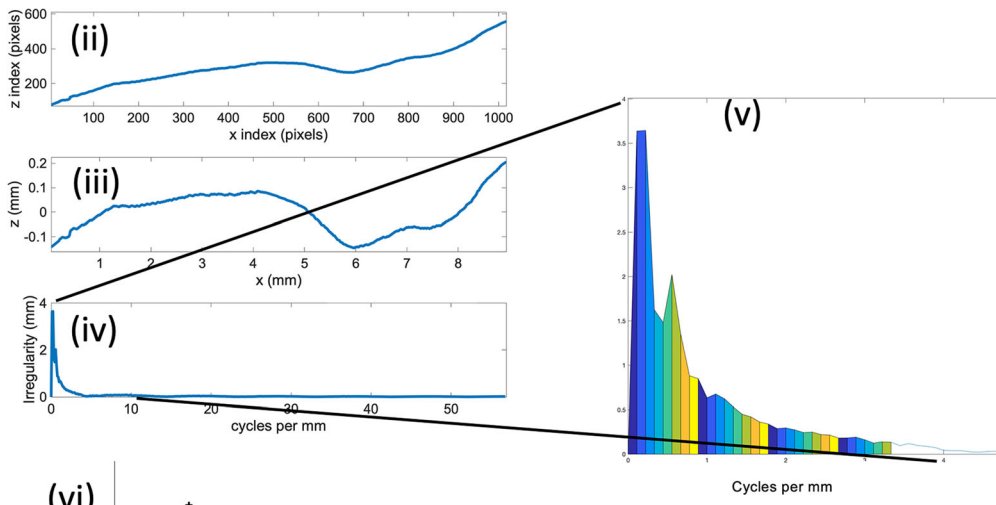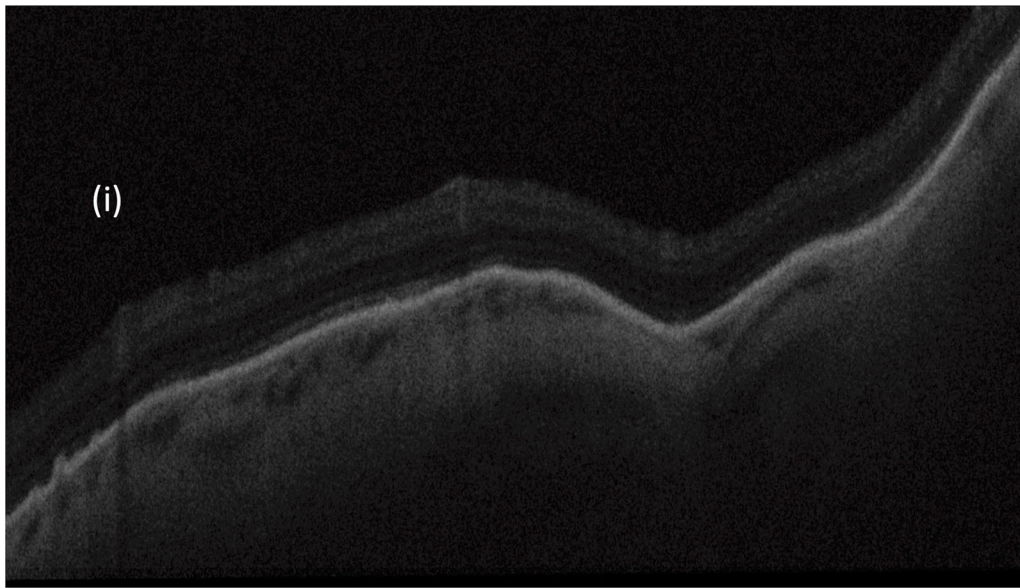
groups, then training an algorithm using these features with a subset of the sample eyes and testing its performance with the remainder of the sample. Training was performed with a randomly selected sample equivalent to 40% of the retinal detachment and PVD eyes, with the remaining 60% as a validation set. The training set was used for feature selection, with all bin values from all regions considered, corresponding to 30 (bins) × 17 (regions) = 510 potential features. The average irregularity was determined for each region of the eye for each group (see Supplementary information 1 and Figure S2). Candidate features selected were those potential features with the greatest difference in average irregularity between retinal detachment and PVD eyes. Axial length was included as a classifier feature as it is known to be associated with both irregularity [12] and risk of retinal detachment [11]. Classifiers were generated with quadratic discriminant analysis [13], a computationally efficient machine learning algorithm, using the PVD and retinal detachment groups as diagnostic classes. With a sample size N, only classifiers with no more than $1 + \log_{10} N$ features were considered suitable [14]. This reduces both the complexity of the model and the risk of overfitting and poor performance. Classifier sensitivity and specificity were calculated with the PVD and retinal detachment eye validation set. Sensitivity was calculated as retinal detachment eyes labelled 2 (true positive) divided by total number of validation set retinal detachment eyes. Specificity was computed as the number of PVD eyes labelled 1 (true negative) divided by the total number of validation set PVD eyes [15]. All permutations of the candidate features were explored to identify the combination with the highest sensitivity that maintained a specificity over 85%, using the training set. This is a stricter test than using re-substitution error, and was chosen as specificity was considered important to minimise the labelling of non-pathological PVD eyes as abnormal. The classifier was further tested with the set of retinal tear eyes.

RESULTS

Feature Selection and Classifier Generation

Initial candidate feature selection found the greatest differences in irregularity between PVD and retinal detachment eyes were all in the supero-temporal hemisphere: post-equatorial

Table 2 Average and standard deviation of irregularity features by diagnosis

	Region 3 – bin 2	SD	Region 5 – bin 3	SD
PVD	0.49	0.26	0.8	0.5
Retinal detachment	0.70*	0.51	1.12*	0.96
Retinal tear	0.58	0.34	0.9	0.58
All eyes	0.59	0.39	0.94	0.72

*Two-sample t-test was significant at $p < 0.05$ for comparison of retinal detachment and PVD irregularity features presented here. There were no significant differences for these features between PVD and retinal tear, or retinal tear and retinal detachment irregularity. Units are mm. *SD* standard deviation

Table 3 Test set confusion matrix

Category	Label 1	Label 2	Total
PVD	*44*	*8*	52
Retinal detachment	*41*	*23*	64
Retinal tear	52	16	68
Total	137	47	184

Performance of the three-variable classifier on the test set of retinal detachment and PVD eyes. The classifier had a sensitivity = 35% and specificity = 84% for identifying retinal detachment eyes. Fisher's exact two-tailed test, comparing PVD and RD distribution (numbers in italics) $p = 0.02$. Label 1 is classifier-predicted class PVD and label 2 is classifier-predicted retinal detachment. The retinal tear eyes are reported in the bottom row as an independent validation set, and were preserved as a distinct category but tested with the same classifier owing to their distinct clinical presentation but similar pathology. *PVD* posterior vitreous detachment
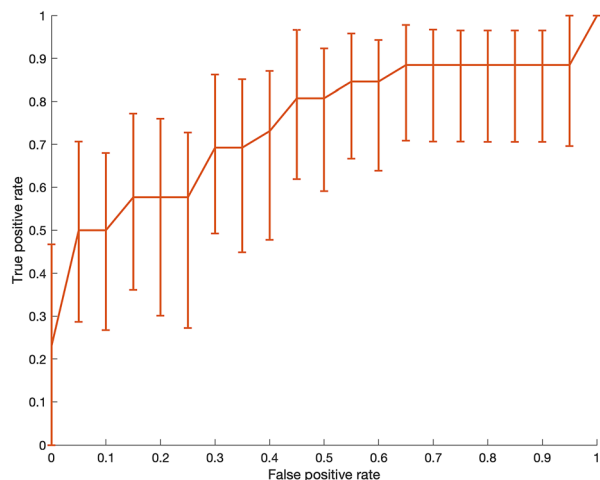
Fig. 3 Receiver operating characteristic curve. For identification of retinal detachment eyes. Error bars representing 95% confidence intervals (CI) were generated from 5000 bootstrap replicas. Area under the curve = 0.75 (95% CI 0.58–0.85)

superior retina (region 3), peri-macular and post-equatorial infero-temporal retina (regions 8 and 9), peri-macular and post-equatorial supero-temporal retina (4 and 5), peri-macular temporal (6) and peri-macular supero-nasal [16] retina. All were from the second and third (lower frequency) bins, corresponding to frequencies of 0.11—0.22 cycles mm^{-1} (bin 2) and 0.22—0.33 cycles mm^{-1} (bin 3), equivalent to feature wavelengths of 3–9 mm. Where two regions in any gaze direction both held candidate features, the post-equatorial regions were selected as they consistently had more irregular scans. As a result, bins from regions 3, 5, 6, 9 and 16 were explored along with axial length by assessing training set classifier performance on all possible three-variable classifier combinations. The most effective three-variable classifier used features from the superior (region 3) and supero-temporal (region 5) regions of the eye, along with axial length. The average values of these features are presented in Table 2. Twenty repeats of fivefold cross validation of the classifier performance with the training set produced an average success rate (true positive + true negative divided by total number of eyes) of 0.69, with a standard deviation of 0.09.

Age was considered as well as axial length. Age had no effect on classifier performance. Single-variable classification using axial length alone varied by the threshold axial length chosen to separate PVD and retinal detachment. At a specificity of 75%, sensitivity was less than 5%, and with a sensitivity of 40%, specificity was only 34%, indicating that axial length on its own was ineffective at identifying retinal detachment eyes.

Test Set Results

The test set confusion matrix is presented in Table 3. Classifier specificity was 84% and sensitivity 35%. A receiver operating characteristic (ROC) curve for identification of retinal detachment eyes, with 95% confidence intervals generated from 5000 bootstrap replicas is shown in Fig. 3, with an area under the curve = 0.75 (95% confidence intervals 0.58–0.85). An ROC curve is a standard device for summarising the performance of a classification system in terms of sensitivity and specificity over the full range of possible operating points [16].

Independent Validation Set

The retinal tear group eyes were used as an independent validation set for the classifier, with these eyes treated as having the same pathology, albeit less advanced disease than retinal detachment. Sixteen eyes (24%) out of 68 in this retinal tear group were labelled '2' (true positive). While retinal tear group features were on average smaller than those of the retinal detachment group, this was only significant for axial length (Tables 1 and 2).

The Effect of PVD and Surgery on Retinal Shape

Two eyes were imaged prior to PVD, and again after PVD occurred. Shape features (20 frequency bins for each of the 17 regions) from the two imaging sessions were compared by a Bland–Altman plot to assess shape metric consistency before and after PVD [e.g. Fig. 4(i)]. The

(i)   (ii)
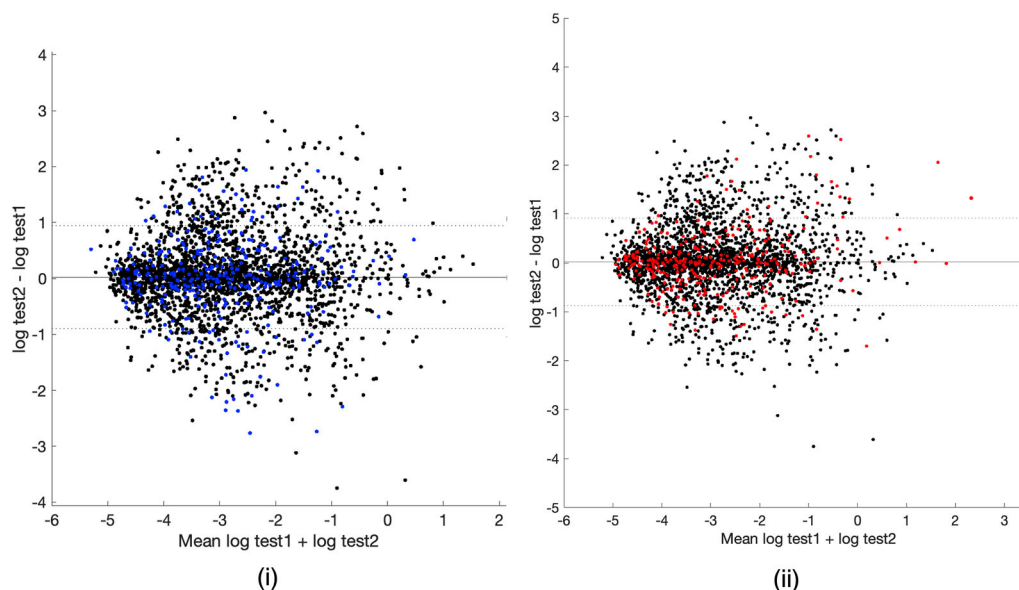
Fig. 4 Bland–Altman test–retest plots of shape metrics (17 regions, frequency bin moduli 2–20) from B scan irregularity spectra before and after PVD [blue points (i)], and before PVD and after vitrectomy for retinal detachment [red points (ii)]. The 95% limits of agreement are set by test–retest measurements from eight eyes with no change in status between examinations (black points). As higher frequency bins and bin 1 are of very low magnitude, only bins 2–20 were plotted to reduce the impact of noise on the plot. Shape metric variation before and after PVD and retinal detachment was no greater than test–retest variation in the absence of any change in ocular condition

95% limits of agreement were generated using eight eyes not included in the main study that had been imaged twice (on separate days) with no change in status between imaging sessions. There was no difference in shape metric variation before and after PVD compared with shape metric variation in eyes with no change in ocular status. Another two eyes were imaged before PVD occurred, and after vitrectomy for PVD-related retinal detachment. Again, the test–retest distribution of shape metrics of these eyes in the Bland–Altman plot matched that of the control eyes [e.g. Fig. 4(ii)]. The two PVD eyes and one of the retinal detachment eyes were labelled '1' when tested with the classifier. The second retinal detachment eye was labelled '2'. Classification label for all four remained unchanged across the two imaging sessions of each eye.

DISCUSSION

With laser treatment known to prevent retinal detachment in some eyes, there is a need for a test to identify more at-risk eyes to reduce the need for emergency surgery and prevent vision loss. This report identifies a potential biomarker, specifically irregularities in retinal shape quantified in the frequency domain, for retinal detachment. These irregularities, used to develop a classifier, were capable of distinguishing between eyes that had suffered a retinal detachment from those that had suffered a PVD.

A sensitivity of 35% is not high (Table 3), but if this performance were to remain the same for eyes at risk of retinal detachment before PVD, it would make one-third of retinal detachments potentially preventable, when at present very few can be targeted with prophylaxis. Evidence presented here that this may be possible was seen with no classification change and no substantive change in shape metrics in two eyes imaged before and after PVD, and two eyes imaged before PVD and after surgery for retinal detachment. The high specificity (84%) gives confidence that an eye labelled '2' was a true positive, crucial were the classifier to be used for prediction or to guide counselling or

intervention. Axial length alone was ineffective at identifying retinal detachment eyes, with the retinal irregularity essential for specificity. Spectral domain OCT is widely available in optometric and ophthalmic practices, and imaging and analysis were fast enough to be practical as a point-of-care test.

The retinal tear group was used as an independent validation set for the two-class classifier. Separation was maintained between retinal tear and retinal detachment eyes to maintain a clean data set, and to explore feature differences between the retinal tear and detachment eyes that might provide evidence as to why these patients present at an earlier stage of the disease than others. In this sample, retinal tear eyes had an axial length significantly shorter than retinal detachment eyes, and longer than PVD eyes. The average age and irregularity of the retinal tear group were also between that of the PVD and retinal detachment groups, but not significantly different from either (Tables 1, 2). This may reflect either that they were a less severe pathology than the retinal detachment eyes, or that they consisted of a mixed group of eyes, some of which would progress to retinal detachment and some of which would not.

Discriminant analysis was developed for Gaussian data, but remains a robust method when this condition is not met, and is a suitable model for this sample size [17]. All machine learning algorithms perform better with larger data sets. The sample presented here was of moderate size, and the use of the training set for feature selection was an effective use of data [14]. This work differs from many applications of machine learning in ophthalmology, which aim to automate the task of a human operator. Instead, it used machine learning tools to identify a new clinical feature. There remain many limitations to this study. Currently OCT can only sample the retinal shape. A more complete morphological analysis, including different scan directions, sample lengths or retinal areas not accessible with this approach might improve classification. Other parameters may predict retinal detachment. Di Michele et al. present a theoretical model that implies the shape of the posterior hyaloid face may differ with different pathological states, which

may be an alternative method of identifying eyes at risk with OCT [18]. Larger samples would allow more complex algorithms to be explored. Patients were all from the age range when PVD or retinal detachments commonly occur, and as eye shape will change over time, the use of the classifier should at present be limited to this age group. All tests need to be used judiciously, as performance depends upon the population studied. Prospective data will be required to investigate whether these features can be used to predict retinal detachment before PVD has occurred, work now being undertaken for the fellow eyes (no PVD) of individuals who have had a retinal tear or detachment in the other eye.

CONCLUSION

The objective was to look for features (in post hoc eyes) that may be present prior to PVD and retinal detachment occurring, that could be explored as a test for retinal detachment in pre-PVD at-risk eyes. Differences in retinal irregularity were found between retinal detachment and PVD eyes. These differences were combined with axial length to train a classifier, which was able to distinguish retinal detachment eyes from PVD eyes. The features were unchanged by PVD itself or retinal detachment surgery in a subset of four eyes imaged before and after PVD and retinal detachment. Prospective evaluation of this test will be undertaken to determine if the test is reliable when performed prior to PVD and disease development.

ACKNOWLEDGEMENTS

Stewart Lake drafted the manuscript and Murk Bottema, Tyra Lange, Keryn Williams, and Karen J Reynolds were involved in editing and revisions to this. Tyra Lange wrote a graph theory algorithm for image analysis.

Disclosures. Stewart Lake, Murk J Bottema, Keryn A Williams, Tyra Lange and Karen J Reynolds confirm that they have no competing interests to declare.

Compliance with Ethics Guidelines. The study was approved by the Southern Adelaide Local Health Network Human Research Ethics Committee (LNR 31.17) and was performed in accordance with the tenets of the Declaration of Helsinki. Prior written informed consent was obtained from all participants.

Data Availability. Code written for this article, and the image data used in the analyses are available from the corresponding author on reasonable request.

Open Access. This article is licensed under a Creative Commons Attribution-NonCommercial 4.0 International License, which permits any non-commercial use, sharing, adaptation, distribution and reproduction in any medium or format, as long as you give appropriate credit to the original author(s) and the source, provide a link to the Creative Commons licence, and indicate if changes were made. The images or other third party material in this article are included in the article's Creative Commons licence, unless indicated otherwise in a credit line to the material. If material is not included in the article's Creative Commons licence and your intended use is not permitted by statutory regulation or exceeds the permitted use, you will need to obtain permission directly from the copyright holder. To view a copy of this licence, visit http://creativecommons.org/licenses/by-nc/4.0/.

REFERENCES

1. Mitry D, Charteris DG, Yorston D, Siddiqui MAR, Campbell H, Murphy A-L, et al. The Epidemiology and Socioeconomic Associations of Retinal Detachment in Scotland: A Two-Year Prospective Population-Based Study. Invest Ophthalmol Vis Sci. 2010;51(10):4963–8. Available from: http://dx.doi.org/https://doi.org/10.1167/iovs.10-5400

2. Howie AR, Darian-Smith E, Allen PL, Vote BJ. Whole population incidences of patients presenting with rhegmatogenous retinal detachments within Tasmania, Australia. Clin Experiment Ophthalmol. 2016;44(2):144–6. Available from: http://dx.doi.org/https://doi.org/10.1111/ceo.12640

3. Polkinghorne PJ, Craig JP. Northern New Zealand Rhegmatogenous Retinal Detachment Study: epidemiology and risk factors. Clin Experiment Ophthalmol. 2004 Jan 1;32(2):159–63. Available from: https://doi.org/10.1111/j.1442-9071.2004.00003.x

4. Geiger M, Smith JM, Lynch A, Patnaik JL, Oliver SCN, Dixon JA, et al. Predictors for recovery of macular function after surgery for primary macula-off rhegmatogenous retinal detachment. Int Ophthalmol. 2020;40(3):609–16.

5. Shunmugam M, Shah AN, Hysi PG, Williamson TH. The Pattern and Distribution of Retinal Breaks in Eyes With Rhegmatogenous Retinal Detachment. Am J Ophthalmol. 2014 Jan 1;157(1):221–6. Available from: https://doi.org/10.1016/j.ajo.2013.09.011

6. Thelen U, Amler S, Osada N, Gerding H. Outcome of surgery after macula-off retinal detachment – results from MUSTARD, one of the largest databases on buckling surgery in Europe. Results from a large German case series. Acta Ophthalmol. 2012;90(5):481–6. Available from: https://onlinelibrary.wiley.com/doi/abs/https://doi.org/10.1111/j.1755-3768.2010.01939.x

7. Van de Put MAJ, Hooymans JMM, Los LI. The incidence of rhegmatogenous retinal detachment in the Netherlands. Ophthalmology. 2013;120(3):616–22. Available from: http://www.sciencedirect.com/science/article/pii/S0161642012008603

8. Ripandelli G, Rossi T, Cacciamani A, Scarinci F, Piaggi P, Stirpe M. Laser prophylactic treatment of the fellow eye in giant retinal tears: long-term follow-up. Retina. 2016;36(5):962–6. Available from: https://journals.lww.com/retinajournal/Fulltext/2016/05000/LASER_PROPHYLACTIC_TREATMENT_OF_THE_FELLOW_EYE_IN.16.aspx

9. Wolfensberger TJ, Aylward GW, Leaver PK. Prophylactic 360° cryotherapy in fellow eyes of

patients with spontaneous giant retinal tears. Ophthalmology. 2003;110(6):1175–7. Available from: http://www.sciencedirect.com/science/article/pii/S0161642003002562

10. Ang A, Poulson A V, Goodburn SF, Richards AJ, Scott JD, Snead MP. Retinal detachment and prophylaxis in type 1 Stickler syndrome. Ophthalmology. 2008;115(1):164–8. Available from: http://www.sciencedirect.com/science/article/pii/S0161642007003405

11. Han X, Ong J-S, An J, Craig JE, Gharahkhani P, Hewitt AW, et al. Association of myopia and intraocular pressure with retinal detachment in European descent participants of the UK Biobank cohort: a Mendelian randomization study. JAMA Ophthalmol. 2020;138(6):671–8. Available from: https://doi.org/10.1001/jamaophthalmol.2020.1231

12. Lake S, Bottema M, Williams K, Reynolds K. The correlation between optical coherence tomography retinal shape irregularity and axial length. PLoS One. 2019;14(12).

13. Fisher RA. The use of multiple measurements in taxonomic problems. Ann Eugen. 1936;7(2):179–88.

14. Lu R-S, Dennison E, Denison H, Cooper C, Taylor M, Bottema MJ. Texture analysis based on Gabor filters improves the estimate of bone fracture risk from DXA images. Comput Methods Biomech Biomed Eng Imaging Vis. 2018;6(4):453–64. Available from: https://doi.org/10.1080/21681163.2016.1271726

15. Friedman J, Hastie T, Tibshirani R. The elements of statistical learning. Vol. 1. Springer series in statistics New York; 2001.

16. Inácio V, Rodríguez-Álvarez MX, Gayoso-Diz P. Statistical evaluation of medical tests. Annu Rev Stat Its Appl. 2021 Mar 7;8(1):41–67. Available from: https://doi.org/10.1146/annurev-statistics-040720-022432

17. Bose S, Pal A, SahaRay R, Nayak J. Generalized quadratic discriminant analysis. Pattern Recognit. 2015 Aug;48(8):2676–84. Available from: http://www.sciencedirect.com/science/article/pii/S003132031500076X

18. Di Michele F, Tatone A, Romano MR, Repetto R. A mechanical model of posterior vitreous detachment and generation of vitreoretinal tractions. Biomech Model Mechanobiol. 2020;19(6):2627–41. Available from: https://doi.org/10.1007/s10237-020-01360-1